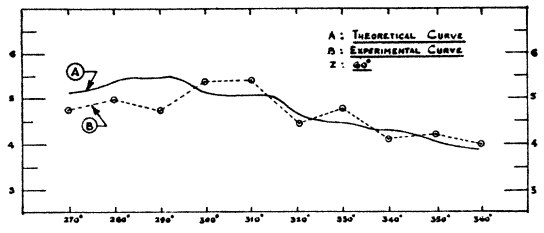

FIG. 1. Azimuthal effect of cosmic radiation in the N-W quadrant at Bombay ($\lambda = 9.5°$N) for zenith angle of 60°.

experimental points shows that though the number of counts at each angle is small, the fit is fairly good, except at azimuth $\alpha = 290°$. On the other hand, the same test shows that the observations are not yet satisfactorily uniform.

It is to be noted that the primary spectrum for energy range from 350 to 640 ms can be represented by K/E^C with $C = 2.45$.

We would like to express our thanks to Professors H. J. Bhabha, M. S. Vallarta, and D. D. Kosambi for their valuable discussion.

[1] M. S. Vallarta, Rev. Mod. Phys. **11**, 239 (1939).
[2] P. S. Gill, Phys. Rev. **67**, 347 (1945).
[3] M. S. Vallarta, M. L. Perusquía, and J. de. Oyarzábal, Phys. Rev. **71**, 393 (1947).
[4] G. Lemaitre and M. S. Vallarta, Phys. Rev. **50**, 493 (1936).

On the Differential Energy Spectrum of Mesons*

M. H. SHAMOS AND M. G. LEVY
Physics Department, New York University, New York, New York
April 13, 1948

THREE points have been obtained in the important low energy region (kinetic energy $<10^9$ ev) of the differential spectrum at sea level by means of a meson detector based upon the instability of mesons. This technique, wherein positive identification of mesons is assured by detection of their decay electrons, has been used by Rossi, Sands, and Sard[1] to investigate the altitude dependence of slow mesons.

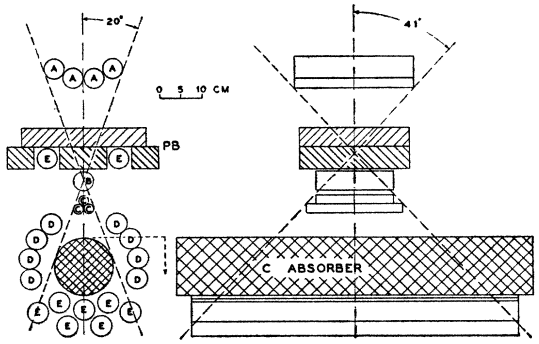

FIG. 1. Counter telescope.

The momentum spectrum of mesons has been investigated with cloud chambers by several workers.[2-5] While the interpretation of such measurements is generally complicated, at low momenta, by the large electron component, Wilson[6] has presented good evidence for a fairly definite maximum in the vicinity of 600 Mev at sea level. However, the usual methods of distinguishing mesons from electrons, such as that based upon the high probability for the production of secondaries by the electrons,[7] are not as reliable as the characteristic decay of the meson.

The counter telescope, shown in Fig. 1, defines a beam (ABC) through the cylindrical carbon absorber, hereafter referred to as "stopper." Counters (E) are connected in anticoincidence and counters (D), effective length 84 cm, detect the decay electrons. The number and distribution in time of the decay events $(ABC-E)(D)$ are recorded by a time circuit somewhat similar to that described by Rossi and Nereson.[8] Because of the time lags in the counters, only those events which are delayed more than 0.95 μsec. are recorded. At this value, the correction for time lags is only $\sim$3 percent.

The meson energies were selected by different thicknesses of absorbing material placed above (A), and between (A) and (B). These thicknesses, taking into account the counter walls (0.5 cm Pb equivalent) and the roof and supporting material in the telescope (0.4 cm Pb equivalent), were: (a) 11.2 cm Pb, (b) 31.6 cm Pb, and (c) 31.6 cm Pb +25.4 cm Fe. The average path length through the absorbing material was evaluated numerically, taking into account the $\cos^2$ distribution of mesons with zenith angle, and found to be 1.1 times the vertical depth. The equivalent cut-off energies, taken from the Rossi-Greisen curves,[9] are then 180 Mev, 465 Mev, and 860 Mev, respectively.

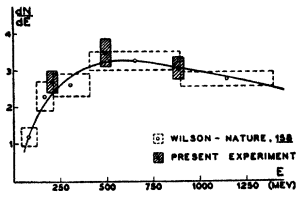

FIG. 2. Differential spectrum.

Runs were taken with and without the carbon stopper under each thickness, and the differences in the numbers of decay electrons were used to determine the differential spectrum. As a check on the experiment, the mean life of the decay process was determined, and was consistent with the value 2.15 μsec. in each case. About 1000 mesons entered the telescope per hour and, of these, some 10 per hour were stopped by the carbon. The pertinent data are tabulated in Table I, where the errors indicated are standard statistical errors.

The differential spectrum is shown in Fig. 2. Here are plotted the relative numbers of decay electrons (in arbitrary units) as a function of the kinetic energy. Since the average path through the carbon stopper is equivalent to about 60 Mev, the points have been located at 210±30

TABLE I.

Absorber thickness	Time (hours) with C	back	Electrons/hour with C	back	Difference per hour	Corrected for time lags
11.2 cm Pb	159.1	152.5	2.41±0.12	0.96±0.08	1.45±0.14	1.42±0.14
31.6 cm Pb	104.1	186.0	3.24±0.17	1.37±0.09	1.87±0.20	1.81±0.20
31.6 cm Pb+ 25.4 cm Fe	135.3	93.7	2.38±0.13	0.74±0.09	1.64±0.16	1.59±0.16

495±30, and 890±30 Mev.** For the purpose of comparison, the point at 890 Mev has been fitted to the Wilson curve, given here on an energy scale; both experiments were performed at approximately the same geomagnetic latitude.

While the statistical errors in this experiment are about the same, or slightly larger than, the errors in Wilson's points, the resolution is sharper, and indicates the usefulness of this technique in the examination of the differential spectrum.

These results were obtained during the course of an investigation into the energy dependence of the positive meson excess, which will be reported on later, and we are indebted to Professor I. S. Lowen for suggesting the initial problem.

* This work was supported by the Office of Naval Research under Contract No. N6ori-201 Task Order II.

[1] Rossi, Sands, and Sard, Phys. Rev. **72**, 120 (1947).
[2] P. Blackett, Proc. Roy. Soc. **A159**, 1 (1937).
[3] H. Jones, Rev. Mod. Phys. **11**, 235 (1939).
[4] D. Hughes, Phys. Rev. **57**, 592 (1940).
[5] E. Williams, Proc. Roy. Soc. **A172**, 194 (1939).
[6] J. Wilson, Nature **158**, 414 (1946).
[7] V. Sarabhai, Phys. Rev. **65**, 203 (1944); **65**, 250 (1944).
[8] Rossi and Nereson, Rev. Sci. Inst. **17**, 65 (1946).
[9] Rossi and Greisen, Rev. Mod. Phys. **13**, 240 (1941).

** This does not take into account the possible spread in energy resulting from the distribution in path lengths through the upper absorber. If the deviations attributable to this effect are taken to be independent of those due to the stopper, the *maximum* energy spread at each point becomes: 210±40, 495±80, and 890±140 Mev. Inasmuch as qualitative considerations indicate that the true spread is much closer to those shown on the diagram than to the maximum, it was decided to show the former rather than the maximum spread. It should be noted, however, that even with the latter, the conclusion given above concerning the improved resolution remains valid.

On Two Complementary Diffraction Problems

A. STORRUSTE AND H. WERGELAND
Norges Tekniske Högskole, Trondheim, Norway
April 20, 1948

OCCASIONED by a discussion on Babinet's theorem, we have worked out exact solutions for the diffraction of sound waves by a circular disk, and in the corresponding hole, *i*, an infinite plane screen.[1]

Two such complementary obstacles are quite different in topological respect, one being singly connected and the other doubly connected. Therefore the mathematical expressions for the diffracted waves will also be entirely different in the two cases.

So Babinet's theorem does not at all emerge simply from the exact solution. It is a limiting principle, like the Huygens-Kirchhoff method on which it is based, valid at short wave-lengths.

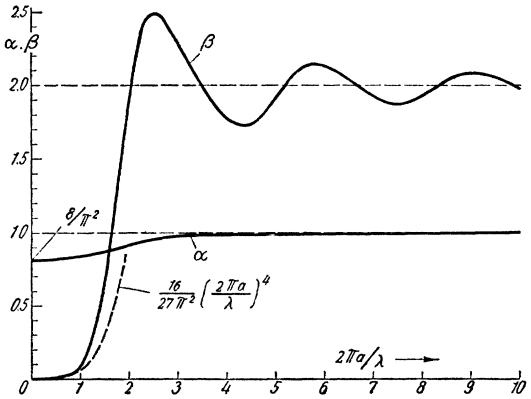

FIG. 1.

The most direct approach to an exact solution is the introduction of spheroidal coordinates. If these—μ, ν, ϕ—are defined by

$$x+iy=a((1+\mu^2)(1-\nu^2))^{\frac{1}{2}}\cdot e^{i\varphi},$$
$$z=a\mu\nu,$$

where

$$a=\text{radius of the hole},$$

the disk and the screen, in the xy-plane, will coincide with the coordinate surfaces $\mu=0$ and $\nu=0$, respectively.

Developing the whole sound field ϕ in the corresponding wave functions

$$\phi_\Lambda=M_\Lambda(\mu)N_\Lambda(\nu),$$

where $\mathbf{N}$ and $\mathbf{\Lambda}$ denote eigenfunctions and eigenvalues of the angular differential equation:

$$(d/d\nu)[(1-\nu^2)(dN/d\nu)]+(k^2a^2\nu^2-\Lambda)N=0,$$

and utilizing integral representations of the form (plane waves):

$$M_\Lambda(\mu)=\int \exp(ika\mu\nu)N_\Lambda(\nu)d\nu,$$

it is easy to write down compact expressions for the wave field satisfying the boundary conditions.

In the numerical elaboration of the results use has been made of the tables of Stratton *et al.*[2] and especially of earlier work of Hylleraas.[3]

We shall here give only the result for the total energy scattered by the disk or transmitted through the hole (Fig. 1).

$$\left.\begin{matrix}\alpha\\ \beta\end{matrix}\right\}=\text{total energy}\left\{\begin{matrix}\text{transmitted}\\ \text{scattered}\end{matrix}\right\}\Big/\,\pi a^2\cdot\text{intensity of primary wave};$$
$\lambda=$ wave-length;
$a=$ radius of hole and disk.

The transmission coefficient, α, starts at a value of 81 percent for long wave-lengths, and the scattering coefficient β increases of course from zero $\sim 1/\lambda^4$ according to Rayleigh's law.

Babinet's theorem applies to the region $\lambda \ll a$, where both curves deviate negligibly from their asymptotes $\alpha=1$, $\beta=2$.